

Indium and gallium on Si(001): A closer look at the parallel dimer structure

M. M. R. Evans

Department of Chemical Engineering and Materials Science, University of Minnesota, Minneapolis, Minnesota 55455-0132

J. Nogami*

Department of Materials Science and Mechanics, Michigan State University, East Lansing, Michigan 48824

(Received 29 October 1998)

Indium and gallium have been shown to self-assemble on the surface of Si(001) into long single atom wide chains in a structure known as the parallel dimer structure. Previous theoretical studies of the similar Al/Si(001) system have calculated the energy of the structure, simulated scanning tunneling microscopy (STM) images, and proposed a nucleation mechanism for row growth. These proposals are compared with STM data for In and Ga. [S0163-1829(99)10711-2]

I. INTRODUCTION

Many scanning tunneling microscopy (STM) studies have been done on the growth of group-III metals on the Si(001) surface,¹ such as Al,^{2,3} Ga,⁴⁻⁶ and In.⁷⁻⁹ These studies have shown that the metal adatoms self-assemble into long chains on the surface of Si(001), perpendicular to the underlying silicon dimer rows. The structure of the adatom rows, known as the parallel dimer structure, has been shown to be the lowest-energy arrangement by several groups.¹⁰⁻¹³ In particular, the work of Brocks, Kelly, and Car (BKC) examines Al on Si(001) in detail.¹⁰ In addition to predicting the lowest-energy structure, they calculate the spatial distribution of electronic states and propose a specific mechanism for row growth.

In this paper STM data for Ga and In adatom rows is compared to the theoretical predictions for Al. Similarities and differences in behavior between the three metals are discussed. Also presented is the observed growth mechanism for these group-III metals.

II. EXPERIMENT

The Si(001) substrates were prepared by flashing the wafers to at least 1200 °C for 30 sec, holding them at 1000 °C for 10 min, then cooling over 10 min. This gave a clean 2×1 surface, as seen by low-energy electron diffraction (LEED) and STM. Ga and In were evaporated from W baskets. Deposition rates were recorded for most experiments with a crystal thickness monitor which gave readings between 0.05 and 0.25 ML/min at the sample. 1 ML = 6.78×10^{14} atoms/cm² for Si(001). Coverages were determined by timed exposures to the sample. The experiments took place in a UHV chamber with a base pressure of 1×10^{-10} Torr, equipped with both LEED and STM.¹⁴ All depositions and STM imaging were done at room temperature (RT).

III. RESULTS AND DISCUSSION

A. Parallel dimer structure

Ga and In form one-dimensional chains on the Si(001) surface at low coverages. Figure 1 shows filled-state STM

images of 0.04 ML of In on Si(001) (upper panel) and 0.09 ML of Ga on Si(001) (lower panel). The rows of In and Ga are brighter features that run from lower left to upper right, and the Si dimer rows run from upper left to lower right. The dark areas on the surface are vacancy defects in the Si(001) substrate which can limit the length of the rows on the surface. Ga, In, and Al, all group-III metals, form these long rows on the Si(001) surface.

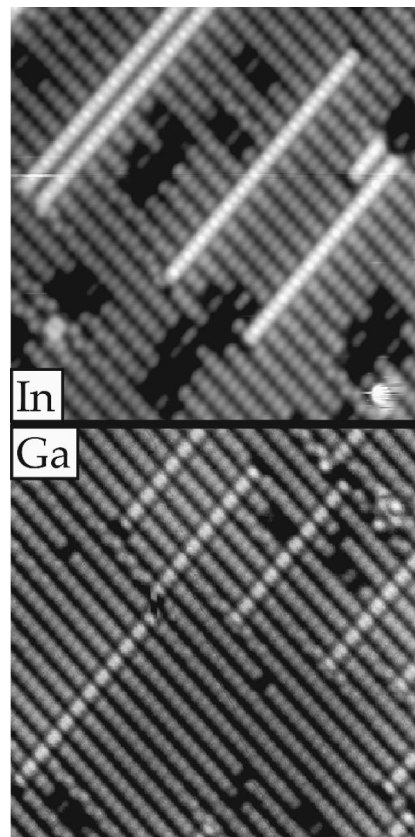


FIG. 1. Low coverage of In/Si(001) and Ga/Si(001). Filled states images of 0.04 ML of In on Si(001), upper, and 0.09 ML of Ga on Si(001). The metal dimer rows run from lower left to upper right, and the underlying Si rows run from upper left to lower right. Several different row terminations are observed ($150 \times 150 \text{ \AA}$).

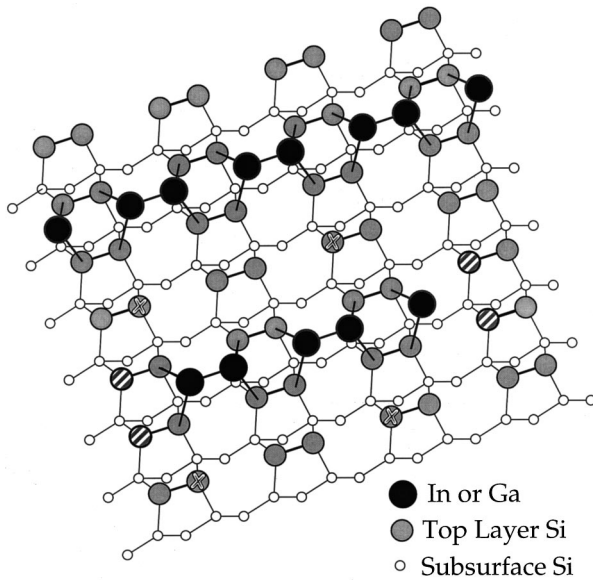


FIG. 2. Parallel dimer model. Si(001) 2×1 dimer rows (gray) run top to bottom, and the metal adatom dimers, either Ga, Al, or In (black) forming the parallel dimer structure, run left to right.

Within these rows the atoms are known to lie in the parallel dimer structure.^{3,10,12,13,15-19} A model of this structure is shown in Fig. 2. The Si dimer rows run up and down in this figure, with the Ga or In rows running from left to right. The metal adatoms arrange themselves into long single atom wide chains of metal dimers running perpendicular to the underlying Si rows, with the individual metal dimers oriented parallel to the underlying Si dimers. The minimum allowable spacing between the rows of In or Ga is $2a$ (where $1a = 1 \times 1$ unit-cell spacing of the Si(001) = 3.84 Å).

There is significant asymmetry between the filled and empty states images of these metal rows. Figure 3 shows

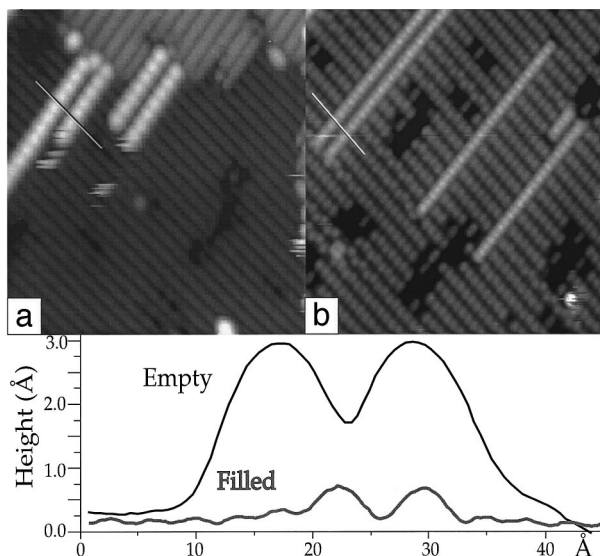


FIG. 3. Filled and empty states of In/Si(001). The heights of (a) empty and (b) filled states cross sections for the In dimer rows are very different. This is a result of the empty orbital associated with each In adatom [(a), +1.48 V sample bias, 0.83 nA; (b) -1.70 V, 0.09 nA].

both bias polarities for In. The rows in the empty states cross section are spaced $3a$ apart, and the rows in the filled states cross section are spaced $2a$ apart. As can be seen from the cross sections below the images, the empty states profile of the In is much higher than the filled states. This comes from the fact that in the parallel dimer structure each of the metal valence electrons is covalently bonded. Two electrons from the In adatom are shared with the two underlying Si atoms, and one with the neighboring In atom with which it forms the dimer (see Fig. 2). Because the bonding arrangement is sp^3 like, there is a completely empty orbital associated with each In adatom. These are directed away from the surface, and account for the very high profile of the empty-state In dimer. The filled states image picks up the π bond between the In dimers and these are much closer to the Si(001) surface. In this particular figure the two images are not of the same area.

Figure 1 shows filled states images of Ga/Si(001) and In/Si(001). From this figure we see at low coverages of either metal that there are very few instances of rows being spaced $2a$ apart. In fact BKC found that by comparing the energy of one Al chain in a $p(2 \times 4)$ unit cell with that of one Al chain in a $p(2 \times 2)$ unit cell that there was an effective repulsion of 0.1 eV per Al atom between the Al chains. Thus, as we have seen from the low coverage images, the rows of metal do not have a tendency to immediately agglomerate into two-dimensional (2D) areas of the 2×2 structure, but instead spread themselves out forming a sparse arrangement of 1D chains. As the coverage is increased for the group-III metals [Al,² Ga,⁴ and In (Ref. 9)] the density of the rows increase, and the spacing between the metal rows decreases towards $2a$, and at coverages of 0.5 ML the entire surface is covered with a 2×2 periodicity.

B. LDOS simulations versus STM data

One of the more interesting aspects of the STM images for In and Ga is their relative similarity with simulated images produced for another group-III material, Al. BKC show the local density of states (LDOS) of the occupied states in the conduction band for an Al row. We can compare this to our data for Ga and In. Figure 4(a) shows the atomic structure of a single row. The Si dimers (small gray circles) are parallel to the metal dimers (larger black circles) but the Si and metal dimer rows are perpendicular to one another. Figure 4(b) shows a representation of the LDOS for Al from BKC, with the dimer structure superimposed. The LDOS image for Al shows a pair of elongated maxima directly over the Si dimers, and small maxima in between the Si dimer rows.

In the filled-state STM image for Ga, Fig. 4(c), the large maxima lie directly over the Si rows and are split into a double lobed feature. The maxima associated with the Ga follow the LDOS image from Al closely; the only feature lacking is the small maximum located between the Si dimer rows.

The filled-state STM image for In, Fig. 4(d), has a single maxima directly over the Si dimer rows, and higher maxima between the Si dimers (directly over the atomic positions of the In dimers). The locations of the maxima from the image are somewhat similar to the LDOS for Al, and are clearly distinct from the atomic positions of the In in the rows.

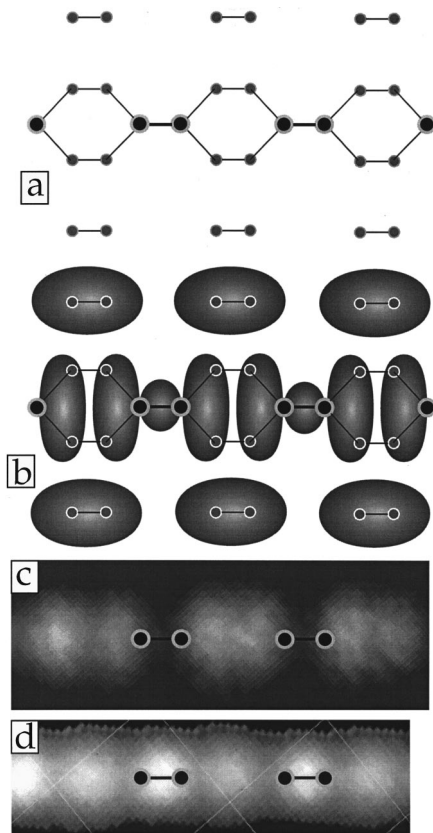


FIG. 4. LDOS vs STM images. (a) Parallel dimer model; (b) a representation of the LDOS of Al with the parallel dimer model superimposed (after Ref. 10); (c) STM image of Ga; (d) STM image of In. Metal adatom dimers are indicated by black circles.

Line profiles provide additional insight into differences between the In and Ga data. Figure 5 shows line profiles taken along rows of In [Fig. 4(d)] and Ga [Fig. 4(c)]. The profiles along the rows of these two metals emphasize the

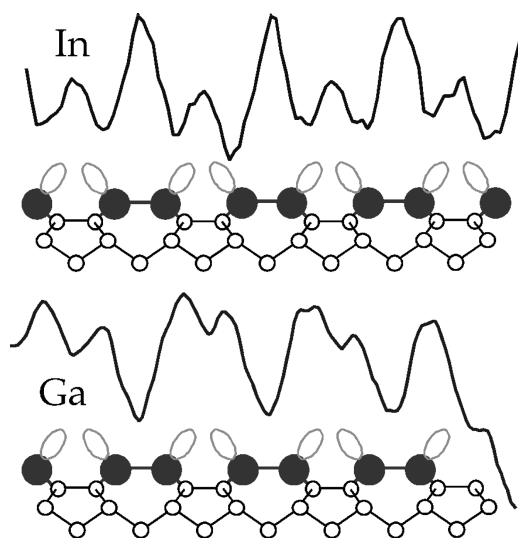


FIG. 5. Cross sections of Ga and In on Si(001). In (top) and Ga (bottom) line scans taken along the dimer row in filled states show the location of maxima in relation to the location of the metal dimers. (In data, -1.70 V, 0.09 nA; Ga data, 0.67 nA, -1.84 V.)

difference we have seen from the STM images. The upper half of Fig. 5 is the line cross section for In in the filled states. The primary maximum occurs over the middle of the In dimer, the location of a double bond, and corresponds to the small round maxima in the simulated image of BKC [Fig. 4(b)]. A secondary maxima occurs between the In dimers, directly over the Si dimer rows. This maxima corresponds to the location of the double lobed structure in the LDOS image, but the shape does not agree with the LDOS. There is some indication that this maxima may be split at certain bias voltages, although this is not readily apparent from the STM images or this cross section. The Ga profile, in the lower half of Fig. 5, has a very different structure. The double lobed maxima from the LDOS image corresponds well to the double lobed maxima located between the Ga dimers. However, the smaller maximum over the metal dimers in the theoretical image is not seen in the STM data.

It is not surprising that the agreement between the data for either metal and the calculated LDOS is not exact. The LDOS calculation is integrated over states in an energy window of 0.5 eV around the valence-band maximum, whereas the STM images shown were taken with tunneling voltages between -1.5 and -2 V.

Overall, the agreement between the Ga data and the Al LDOS is closer than that for In. Of these three group-III metals, Al and Ga might be expected to be more similar since the size of Al and Ga is about the same. Moreover, the bond lengths for Al and Ga in the parallel dimer structure are close to each other and somewhat different than those for In (2.47 Å for the Al and Ga adatom-Si bond, and 2.60 Å for In adatom-Si bond).¹² The data for Ga places maxima in the appropriate positions of atoms in the parallel dimer structure. In this respect, the data is similar to published data for Al.³ However, it is an oversimplification to state that the metal atoms are being resolved by the STM. It is best to state that the STM maxima correspond to maxima in the LDOS, and that these maxima can in general be in different positions than the atoms, as is clearly the case for In.

C. Row ends

Metal rows can have several different types of row ends, as shown in Fig. 6. There are dark ends (D) where the two Si dimers at the end of a Ga row appear to be missing. There are also bright ends (B) where the Si dimers at the end of a Ga row can be seen. These are the most common types of row ends, accounting for over 80% of the counted features. Other row end features include half-bright (H) row ends, as seen in Fig. 6. These features are almost always associated with a row end that is adjacent to a continuing row, as is seen in Fig. 6. The other row end of note is an asymmetric end (A) with a bright feature that is shifted laterally by $\frac{1}{2}a$ from the middle of the Ga row. This asymmetrical end can be seen in the upper right corner of the Ga image in Fig. 1. Of 350 row ends tabulated for the surface shown in Fig. 6, the great majority were of type D ($\frac{142}{350}$ or 41%), or type B ($\frac{150}{350}$ or 43%). The other types accounted for the remaining 17% (H :7% and A :10%). Other row ends directly attributed to missing Si dimer defects accounted for less than 5% of the total row ends and were not counted.

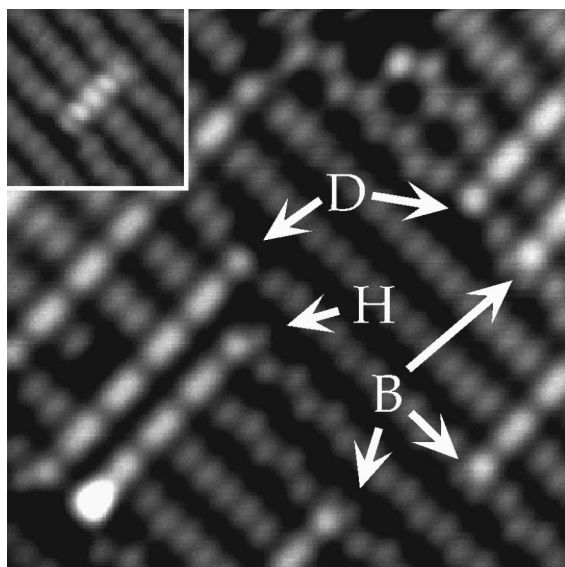


FIG. 6. Row ends. This image shows the row ends for Ga/Si(001). Bright ends (*B*), dark ends (*D*), and half bright ends (*H*) are indicated. The inset shown In/Si(001), and both *B* and *D* row terminations can be seen (filled states).

The ratio of type-*B* to type-*D* row ends is very even. This may lead one to think that one end is associated with a dimer termination, and the other with a single adatom of Ga. There have been LDOS of row ends done for Al/Si(001) by BKC,¹¹ which show the structures for Al dimer row end termination and for a single Al atom at the end of a row. The LDOS images suggest that the type-*B* row ends are associated with a metal dimer termination. However, the LDOS for the single adatom row termination for Al does not agree with our STM images. BKC also predicts that the metal dimer termination should be more common than the monomer, which does not agree with our observations.

If we assign a Ga dimer row end to type *B* and a Ga monomer row end to type *D*, we might expect that in an empty states image type-*B* ends would be darker than type-*D* ends, opposite to what is seen in filled states. Surprisingly, there seems to be very little difference in the appearance of type-*B* and -*D* row ends in the empty states. This may be due to a relaxation of Ga monomers at the row ends. A final understanding of the structure of these row ends will require further theory.

We should note that at either type-*B* or -*D* ends, there is a buckling of the Si dimer row that travels symmetrically along the Si dimer row away from either side of the metal row end. Furthermore, the phase of the buckling is the same for both type-*B* and -*D* row ends and is in the direction where the Si dimers adjacent to the metal row are tilted down away from the direction of the row. Referring to Fig. 2, this would mean that the Si atoms labeled *X* would be buckled upward, and the buckling would continue in the usual alternating manner along the Si dimer row. Note that this has different consequences for the two types of row ends. For type *B*, this means that the last Si atoms to be bonded to a metal dimer atom are pushed down, whereas the Si atoms bonded to a metal monomer would pucker outward.

The inset in Fig. 6 shows a very short row of In with both type-*B* and type-*D* terminations. This demonstrates that al-

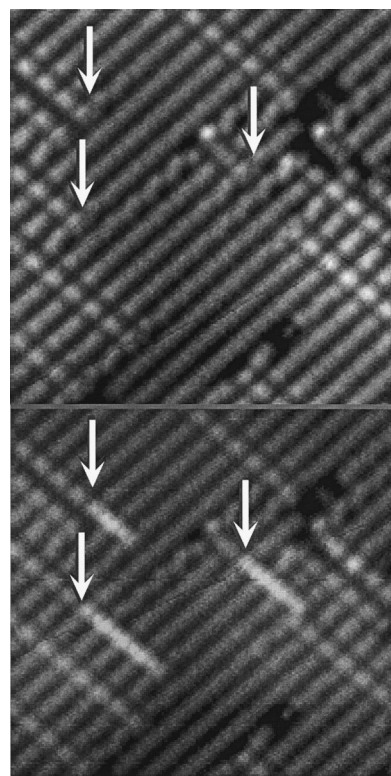


FIG. 7. Growth of In on the ends of Ga rows. *In situ* depositions of In onto a surface already containing Ga rows show that the In preferentially nucleates at the ends of existing Ga rows. The arrows point to the same location in each of the two images (filled states: upper, -1.47 V, 0.23 nA; lower, -1.82 V, 0.23 nA).

though the appearance of the metal within the row differs from the Ga data, both metals show the same types of row ends.

Itoh *et al.*³ have shown similar images of row ends for Al/Si(001). They report that the monomer termination of row ends is more common than the dimer termination. They also report isolated Al monomers that are perhaps stabilized by the presence of nearby defects in the substrate. We do not see these monomers. This could be because of a lower Si defect density, and in any case, the small number of such features would fall into a class that make up less than 5% of the row ends.

D. Row growth

Another prediction of BKC concerned the mechanism for the growth of the one-dimensional rows; there is a strong preference for a third adatom to join a dimer on the surface in a specific location adjacent to the dimer, causing the dimer to grow. A fourth adatom would form a second dimer with the single atom located at the end of the row in order to lower the surface energy. These preferred sites are indicated in Fig. 2 by striped Si atoms. The growth continues from both ends of the metal chain and causes long rows to form. BKC referred to this as a surface polymerization, because of the similarity to reactions taking place with organic polymers.

We can confirm that this type of nucleation is followed by the Ga and In system by depositing a very small amount of In on the Ga/Si(001) surface. Figure 7 shows two images. The top image is of 0.09 ML of Ga on Si(001), with the Ga rows running from upper left to lower right. The bottom

figure shows the same area, after the addition of a very small amount (approximately 5×10^{-5} ML) of In. As noted earlier, the Ga and In are clearly distinguishable in a filled states image. The arrows point to the same places in the upper and lower images. As might be expected, the In continues row growth at the ends of the Ga rows. Also of note is the movement of the buckling of the underlying Si. Buckling is seen at the row ends for Ga/Si(001) in the upper figure. This buckling extends perpendicularly away from the Ga row in both directions, affecting three to five Si dimers. After the In deposition the buckling is no longer located where the ends of the Ga rows are (as indicated by the arrows), but instead the buckling now occurs at the ends of the In rows.

IV. SUMMARY

In and Ga deposited on Si(001) closely follows the theoretical predictions made for Al on Si(001), done by BKC.¹⁰

The simulated STM images for metal atoms in the parallel dimer structure have many of the same features that we have found in our images of Ga and In. Row ends are examined in detail and the nature of different features is discussed. In addition the mechanism of row growth is clearly supported by sequential depositions of Ga and In onto the same area of the sample.

ACKNOWLEDGMENTS

Acknowledgment is made to the Donors of the Petroleum Research Fund, administered by the American Chemical Society, for partial support of this research. The experimental work was carried out at the University of Wisconsin-Milwaukee with partial support from the Laboratory for Surface Studies.

*Corresponding author. FAX: 1-517-353-9842. Electronic address: nogami@egr.msu.edu

¹J. Nogami, in *Atomic and Molecular Wires*, edited by C. Joachim and S. Roth (Kluwer Academic, Dordrecht, 1997), Vol. 341, pp. 11–21.

²J. Nogami, A. Baski, and C. F. Quate, *Phys. Rev. B* **44**, 1415 (1991).

³H. Itoh, J. Itoh, A. Schmid, and T. Ichinokawa, *Phys. Rev. B* **48**, 14 663 (1993).

⁴A. A. Baski, J. Nogami, and C. F. Quate, *J. Vac. Sci. Technol. A* **8**, 245 (1990).

⁵J. Nogami, S.-I. Park, and C. F. Quate, *Appl. Phys. Lett.* **53**, 2086 (1988).

⁶J. Nogami, A. A. Baski, and C. F. Quate, *J. Vac. Sci. Technol. A* **8**, 3520 (1990).

⁷J. Knall, J.-E. Sundgren, G. V. Hansson and J. E. Greene, *Surf. Sci.* **166**, 512 (1986).

⁸A. A. Baski, J. Nogami, and C. F. Quate, *Phys. Rev. B* **43**, 9316 (1991).

⁹A. A. Baski, J. Nogami, and C. F. Quate, *J. Vac. Sci. Technol. A* **9**, 1946 (1991).

¹⁰G. Brocks, P. J. Kelly, and R. Car, *Phys. Rev. Lett.* **70**, 2786 (1993).

¹¹G. Brocks, P. J. Kelly, and R. Car, *J. Vac. Sci. Technol. B* **12**, 2705 (1994).

¹²J. E. Northrup, M. C. Schabel, C. J. Karlsson, and R. I. G. Uhrberg, *Phys. Rev. B* **44**, 13 799 (1991).

¹³G. B. Adams and O. F. Sankey, *J. Vac. Sci. Technol. A* **10**, 2046 (1992).

¹⁴Omicron, Taunusstein, Germany.

¹⁵L. Li, C. Koziol, K. Wurm, Y. Hong, E. Bauer, and I. S. T. Tsong, *Phys. Rev. B* **50**, 10 834 (1994).

¹⁶Y. Qian, M. J. Bedzyk, S. Tang, A. J. Freeman, and G. E. Franklin, *Phys. Rev. Lett.* **73**, 1521 (1994).

¹⁷B. E. Steele, L. Li, J. L. Stevens, and I. S. T. Tsong, *Phys. Rev. B* **47**, 9925 (1993).

¹⁸H. W. Yeom, T. Abukawa, Y. Takakuwa, M. Nakamura, M. Kimura, A. Kakizaki, and S. Kono, *Surf. Sci. Lett.* **321**, L177 (1994).

¹⁹H. W. Yeom, T. Abukawa, M. Nakamura, S. Suzuki, S. Sato, K. Sakamoto, T. Sakamoto, and S. Kono, *Surf. Sci.* **341**, 328 (1995).